1. Introduction

In Japan, most metropolises are on the soft ground in alluvial plain, and pile foundations are often used for substructures. Pile foundations are vulnerable to ground motion in the horizontal direction and can be damaged by the inertial force transmitted from superstructures and the kinematic force induced by the soil displacement along with liquefaction during strong earthquakes. These two forces can be accurately evaluated by the seismic response analysis of a high fidelity model of a soil-structure system, and a finite element method (FEM) enhanced with high performance computing (HPC) is a major component in such seismic response analysis.

With the development of the FEM enhanced with HPC, the three-dimensional (3D) FEM has been adopted in previous studies [1, 2]. Recalling that the 2D analysis involves certain approximations, the superiority of 3D analysis is obvious. However, the two-dimensional (2D) FEM is still the mainstream method in practice. For example, while conducting the 2D liquefaction analysis, a 2D version of FLIP ROSE [3] (***F***inite element analysis program of ***Li***quefaction ***P***rocess / ***R***esponse ***o***f ***S***oil-structure systems during ***E***arthquakes. Hereafter "FLIP 2D") is widely used for practical seismic design in Japan, whereas a 3D version of FLIP ROSE, i.e. FLIP 3D [4], seems rarely used. We consider that a major reason for this is insufficiency of validation of the 3D model.

In this study, we seek to validate a 3D FEM model by comparing the numerical results with the experimental data; the data were measured in E-Defense [5, 6], the largest shaking table in Japan, for a soil-pile-structure system which consisted of piles and structures. The comparison is made for densely measured accelerations and pore water pressures of the pile foundation and the liquefied ground.

In this paper, we first describe the shaking table tests of E-Defense. We explain the settings and results of the numerical analysis for the 3D FEM model. We discuss the results of comparing the numerical analysis with the experimental data. Finally, the concluding remarks are summarized.

2. Shaking table tests

Figure 1 shows the soil-pile-structure system that was used in E-Defense. The system was installed in a cylindrical laminar box with the height and diameter of 6.3 m and 8.0 m, respectively. The laminar box consisted of forty-one stacked ring flames which could slide in the horizontal direction.

The soil consisted of two layers. The first layer was a saturated layer of Albany sand from Australia and the second layer was cement-mixing sand at the bottom of piles. The saturated layer of Albany sand composed of dense and medium-dense sand layers with the relative densities being approximately 90% and 60%, respectively. The water table was 0.5 m below the ground surface.

A 3×3 steel pile group with normalized pile spacing was used for the test. Each pile had a diameter of 152.4 mm, a wall thickness of 2.0 mm, and a length of 5.7 m. The piles were labeled A1 to C3 according to their locations in the pile group, as shown in Fig. 1. The steel footing weighed 10 tons whereas the superstructure made of steel weighted 12 tons. The tips of the piles were joined to the base with pins and pile heads were fixed to a footing with a weight of 10 tons by injecting non-shrinkage cement into the gaps between the footing and the pile.

The tests were conducted under shaking of two horizontal direction with two different ground motions that were recorded at Takatori in 1995 Kobe earthquake and at Akasaki in 2000 Tottori earthquake. Table 1 shows the test conditions of the input motions. The numerical study in this paper is focused on the ground motion of Takatori, the maximum acceleration of which is 3.0 m/s^2, presuming that this strong ground motion induces the soil liquefaction and the nonlinear behavior of the piles. The experiment that used Takatori ground motion was conducted at the end of the test series.

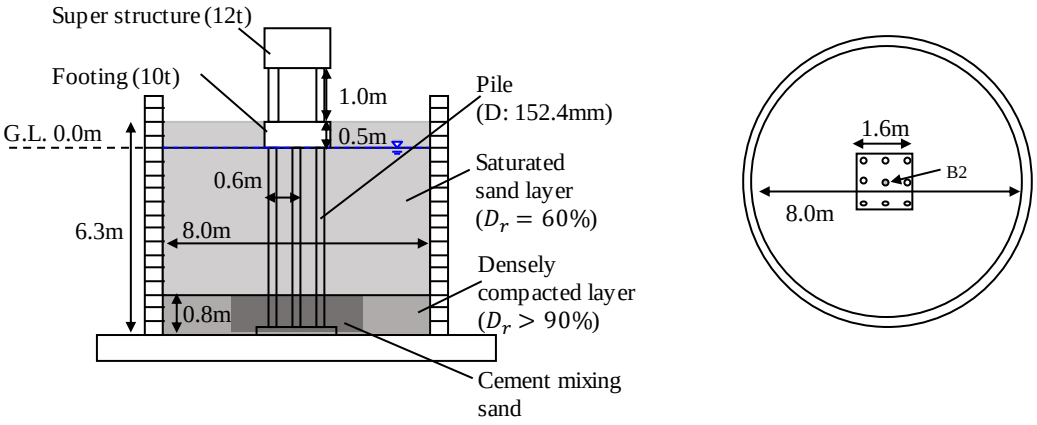

(a) Side view (b) Plan view

Fig. 1 Soil-pile-structure system

Table 1 Test conditions

Input motion	Maximum input acceleration
Tottori	0.3 m/s^2, 0.8 m/s^2, 1.3 m/s^2
Takatori	0.3 m/s^2, 0.8 m/s^2, 3.0 m/s^2

3. Numerical Analysis

3.1 Analysis program

This paper used FLIP 3D (version 1.6), which is a liquefaction analysis program of 3D FEM that uses the Mohr-Coulomb's failure criterion. The governing equation for the FEM analysis is

$$\boldsymbol{Ma} + \boldsymbol{Cv} + \boldsymbol{Ku} = \boldsymbol{f}, \tag{1}$$

where $\boldsymbol{u}$, $\boldsymbol{v}$, $\boldsymbol{a}$, and $\boldsymbol{f}$ are displacement, velocity, acceleration and external force vectors, respectively, and $\boldsymbol{M}$, $\boldsymbol{C}$ and $\boldsymbol{K}$ are (consistent) mass, damping, and stiffness matrices, respectively. We use the stiffness proportional damping for $\boldsymbol{C}$. The time integration employs the Wilson θ method.

In FLIP 3D (version 1.6), a constitutive relationship of the strain space multiple mechanisms is employed for the soil, and an excess pore water pressure model is employed for liquefaction [4]. We implement the parallel direct solver [7] in the original program of FLIP 3D (version 1.6) to enhance it with HPC.

3.2 Analysis model

Figure 2 shows the 3D FEM model; the node number is approximately 140,000; the maximum height of the elements is 0.25 m; and the maximum aspect ratio is 9.2.

The ground is divided into three layers; the first layer above the water table is the dry sand with a relative density, D_r, of 60%; the second layer is the liquefiable saturated sand with $D_r = 60\%$; and the third layer is non-liquefiable saturated sand with $D_r = 90\%$. Tables 2 and 3 summarize the model parameters of the soils; used are the parameters which were measured on the laboratory test of the soil or the in-situ test of the model

of E-Defense. The S-wave velocity profile of the 3D FEM model and the experiment is compared in Fig. 4. Also, the liquefaction strength curve of the cyclic test is compared in Fig. 5.

In the 3D FEM model, the piles are modeled as non-linear beam elements. As shown in Fig. 3, rigid beam elements which connect nodes for the pile and the ground are used in the space inside the pile. The parameters of the piles, such as density and shear stiffness, are specified according to the ordinary parameters of steel, and summarized in Table 4. Parameters for nonlinearity are set based on a yield strength of SKK steel at 235 N/mm^2. The relation between the bending moment and the curvature of the pile subjected to an axial force of 50 kN is illustrated in Fig. 6. The gradient of the curve became 0.05 times smaller after yielding. The effect of the axial force on the nonlinearity is not taken into consideration.

In the E-Defense experiments, the pile heads and footing were tightly fixed by injecting non-shrinkage cement into the gaps between them. The previous studies [8, 9] which numerically analyzed the same structure with different ground conditions showed that the bending strain at the pile heads of the numerical analysis was much higher than the one measured in the experiment. Investigation was made to clarify the cause of this difference by using two approaches. The first approach was to detach a constraint between the pile heads and the bottom of the footing and to allow them to move independently, based on the assumption that the connection by cement at the pile head was loosened by repeated shaking in the previous tests so that the rigidity at the pile heads was decreased (see Fig. 7). The second approach was to consider the rocking motion of whole system and to add vertical springs at the bottom of the laminar box so that the rocking motion was reproduced during the shaking table tests. This paper followed the first approach.

The superstructure and the footing are modeled as linear soil elements and the laminar box frame and column are modeled as linear beam elements. The model parameters of them are set based on the ordinary steel parameters as shown in Table 4.

Figure 8 shows the input ground motion measured at Takatori, the maximum acceleration of which is 3.0 m/s^2. The motions are applied to the bottom of the box in two horizontal directions. We use the Wilson θ method of $\theta = 1.4$ with the time increment of $dt = 0.01$ s. As for the stiffness proportional damping, we use the damping constant of 2% at 7.8 Hz, which was the natural frequency of the pile foundation in the E-Defense experiments.

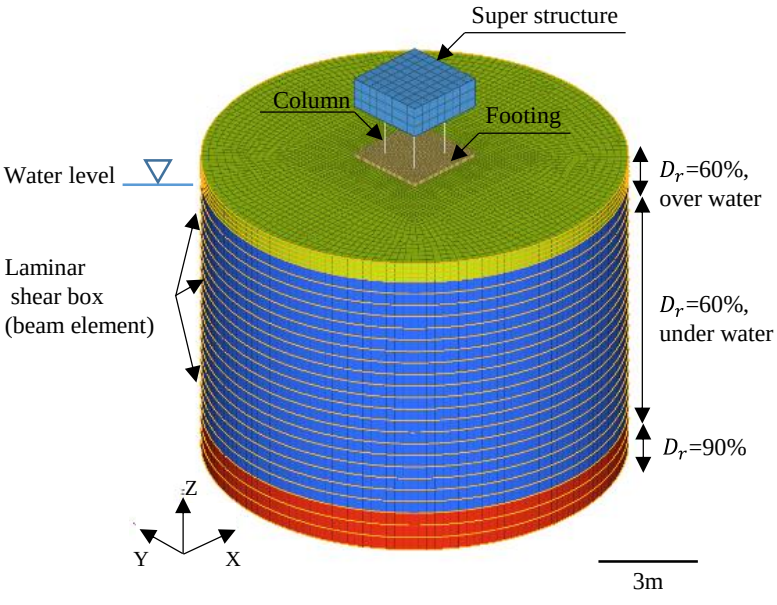

Fig. 2 Analysis model

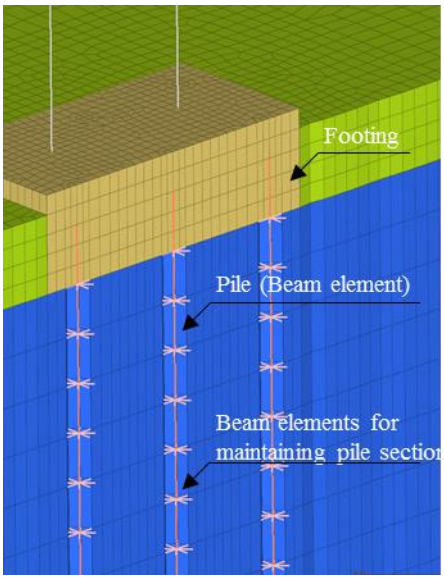

Fig. 3 Details of the pile and footing

Table 2 Parameters for dynamic characteristics of soil

Layer	G.L. (m)	ρ (t/m^3)	V_s (m/s)	G_{ma} (kPa)	σ'_{ma} (kPa)	ν (-)	ϕ_f (deg.)	h_{max} (-)
D_r=60% (dry)	0.0 to -0.5	1.700	160	43520	2.22	0.33	38.7	0.24
D_r=60%	-0.5 to -5.3	2.006	160	51342	21.21	0.33	38.7	0.24
D_r=90%	-5.3 to -6.3	2.058	200	82338	43.36	0.33	38.7	0.24

ρ: density; Vs: shear wave velocity; G_{ma}: the elastic shear modulus at a confining pressure of ($-\sigma'_{ma}$); -σ'_{ma}': the reference confining pressure; and $\sigma'_{ma}=\sigma'_v\cdot(1+2Ko)/3$, where σ'_v: the effective vertical pressure at the center depth of the soil; Ko: coefficient of the earth pressure at rest (K0=0.5); ν: the Poisson's ratio;ϕ_f : the shear resistance angle; and h_{max}: the maximum damping ratio.

Table 3 Parameters for liquefaction

Layer	G.L. (m)	n (-)	K_w (kPa)	ϕ_p (deg.)	S1	w1	p1	p2	c1
D_r=60% (dry)	0.0 to -0.5	-	-	--	-	-	-	-	-
D_r=60%	-0.5 to -5.3	0.383	2200000	28	0.005	7.850	0.500	1.000	3.090
D_r=90%	-5.3 to -6.3	0.383	2200000	-	-	-	-	-	-

n: the voil ratio; ϕ_p: the phase transformation angle; K_w: the bulk modulus of pore water; p1: the initial phase; p2: the final phase; w1: the overall dilatancy; S1: the ultimate limit; and c1: the threshold limit of dilatancy.

Table 4 Parameters for steel

ρ (t/m^3)	G (kPa)	ν (-)
7.45	8.4×10^7	0.25

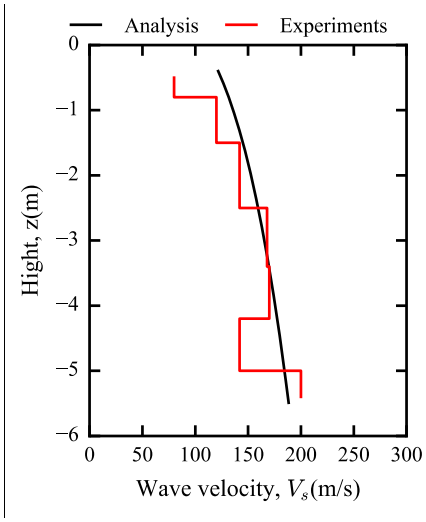

Fig. 4 S-wave velocity

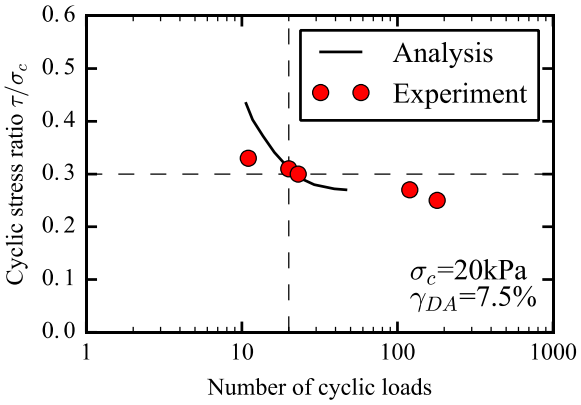

Fig. 5 Cyclic stress ratio versus the number of cycles

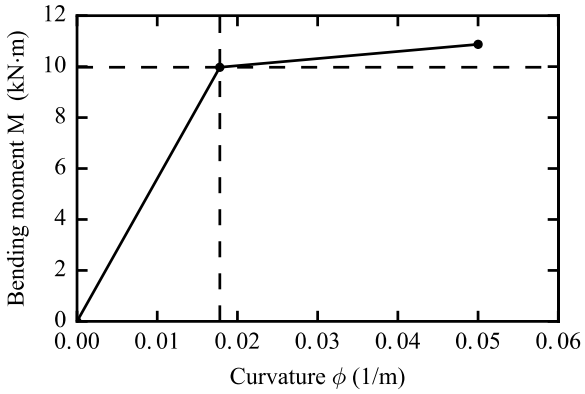

Fig. 6 M-ϕ of the piles

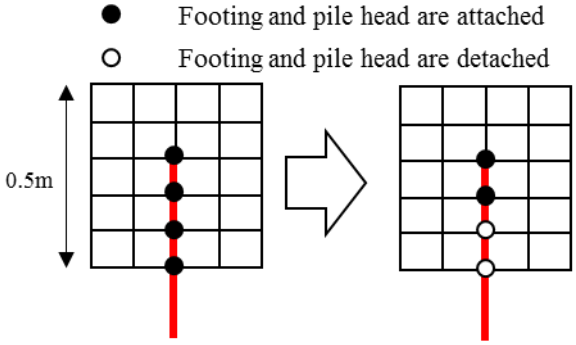

Fig. 7 Constraint of the nodal points at the pile head

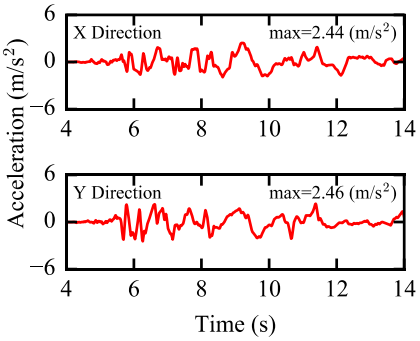

Fig. 8 Input motions

3.2 Results

This section discusses the result of comparisons between the numerical analysis and the experiment.

Figure 9 shows the time history of the pore water pressure. It was found that the numerical analysis could reproduce the experimental results satisfactorily. A fairly well agreement was observed at the instance when the decrease of pore water pressure occurred at 6 s and 7 s. At G.L. -1.0 m, however, the pore water pressure decrease of the experiment was more significant than that of the analysis. It was also found that the fluctuation of pore water pressure around the piles became larger in the analysis than in the experiment after 9 s.

Figure 10 shows the time history of the displacement of the ground. It was shown that the analysis could reproduce the experimental results reasonably well. We suspect that the non-smooth behavior of the displacement at 7 s and 10 s in the experiment was caused by the failure of a laser pointer that missed the target for the displacement measurement.

Figure 11 shows the time history of the acceleration at the superstructure, the footing, and the ground surface. The analysis reproduced the peak of acceleration at 7 s which might have caused the cyclic mobility in the soil. Acceleration at 6 s in the analysis was larger than in the experiment. The reason for this difference might be that the pore water pressure at 6 s in the analysis decreased more significantly than that in the experiment.

Figure 12 shows the time history of the acceleration in the soil. Significant pulse of acceleration was observed in the experiment especially after 8 s. Although such significant pulse were not reproduced by the numerical analysis, the acceleration time history around 7 s was reproduced reasonably well.

Figure 13 shows the maximum bending strain at the pile B2 which was located at the center of the footing. In the experiment, the bending strain was found larger at the pile heads and on the boundary between the layers with $D_r = 60\%$ and $D_r = 90\%$ than the other parts of the pile (GL-0.5m to -3.0m). In the numerical analysis, the bending strain was also found high at the same places. However, the value of the bending strain was more than two times higher than that in the experiment. In addition, more plastic deformation was found in the numerical analysis than in the experiment. Fig. 14 depicts the time history of the bending strains, showing clearly that the bending strain in the numerical analysis was higher than that in the experiment at 10 s and 12 s during the occurrence of liquefaction.

As discussed in Section 3.2, the inconsistency for the bending strain at the pile heads can be caused by the constraint of the pile heads as well as by the effect of rocking motion of whole system. In fact, the rocking motion was observed in the vertical displacement near the bottom of the laminar box, which was computed by integrating the observed vertical accelerations with respect to time. Such vertical movement did not occur in the numerical analysis; see Fig. 15. It may be possible to reduce the inconsistency of bending strain at the pile heads by placing vertical springs at the bottom of the box to initiate rocking motion, as described in the previous studies [8, 9]. However, there is no widely accepted approach to specify the stiffness of the vertical springs.

The bending strain of pile at the soil layer boundary can be induced by the difference of the stiffness for the two layers. In the numerical analysis, the distinct material parameters were used for the two layers, and the pore water pressure time history was clearly different. On the other hand, in the experiment, the boundary was thought to be vague, and the stiffness was found to change gradually in the vertical direction; therefore, the bending strain of piles at the boundary was larger in the analysis. If a 3D FEM model with a larger number of layers was used and the soil stiffness was changed gradually in the vertical direction, the analysis could reproduce the experiment more consistently.

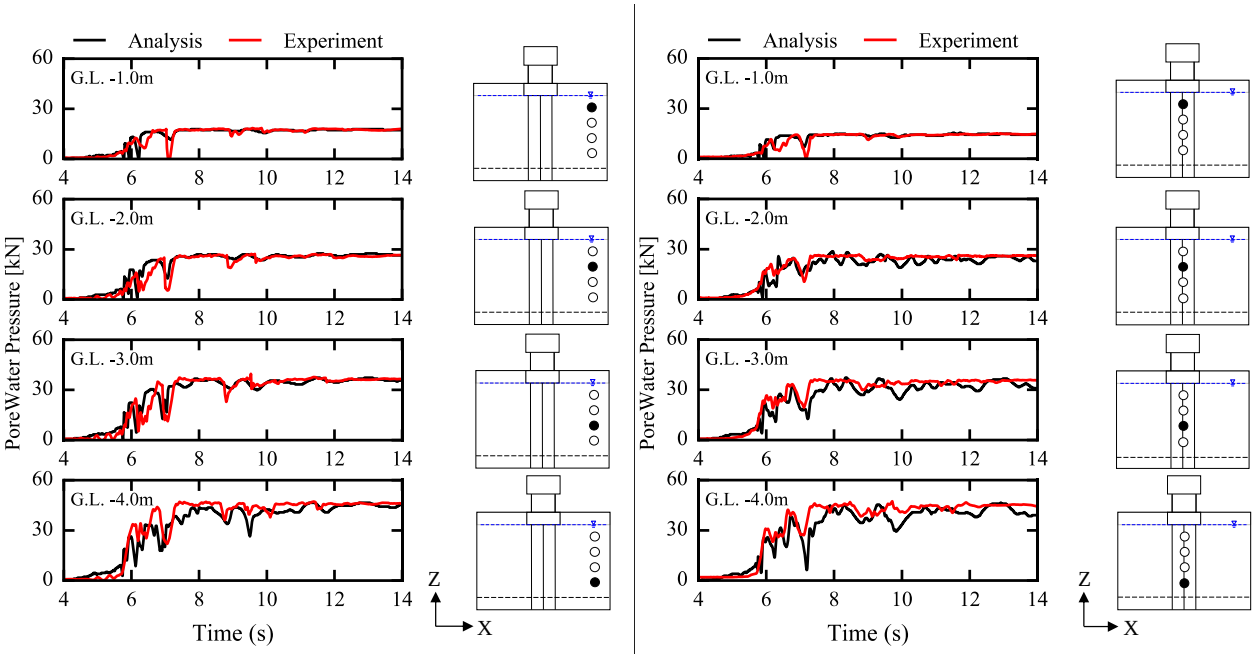

(a) Around the box (b) Around the piles

Fig. 9 Time histories of the pore water pressure

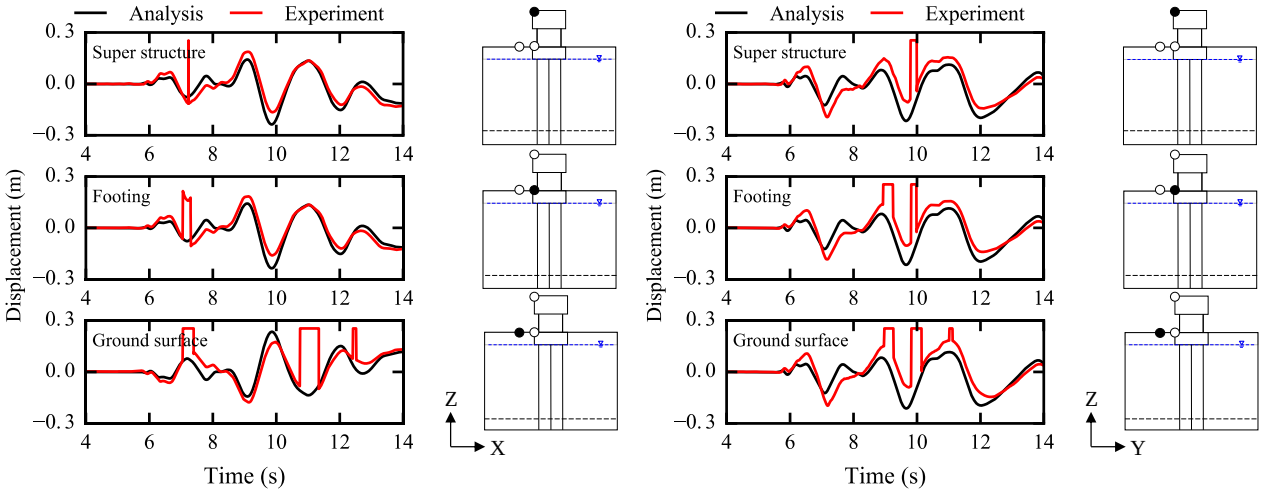

(a) *X*-direction (b) *Y*-direction

Fig. 10 Time histories of the horizontal displacement

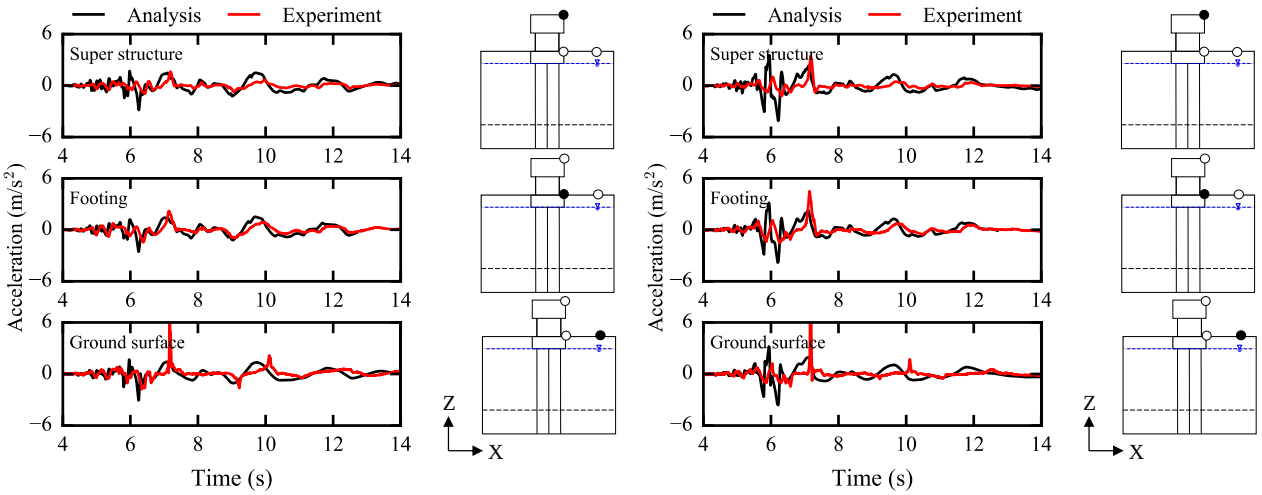

(a) *X*-direction (b) *Y*-direction

Fig. 11 Time histories of the acceleration (super structure, footing, and ground surface)

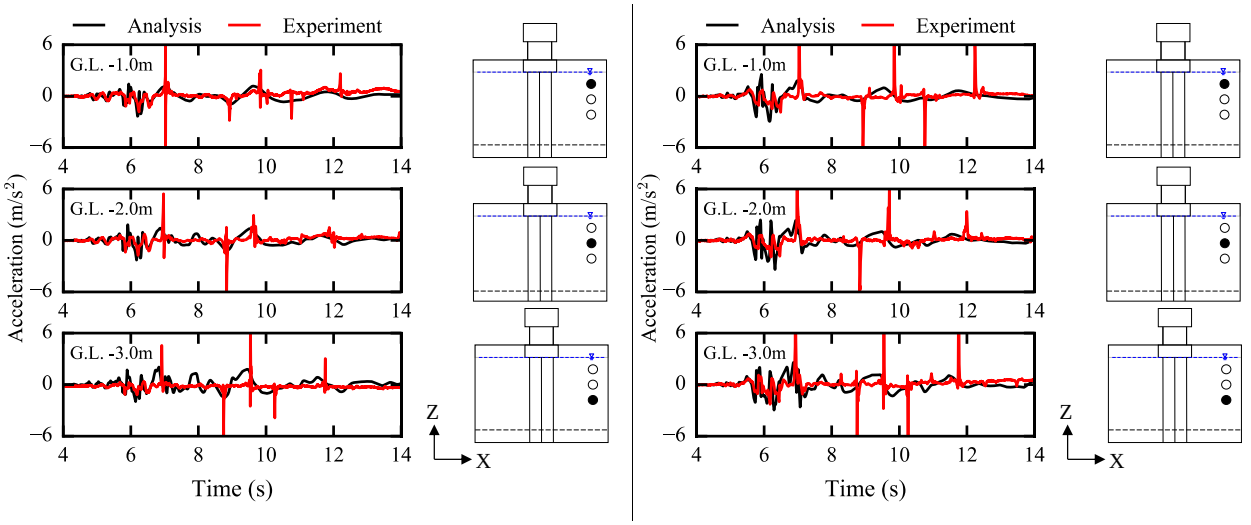

(a) *X*-direction (b) *Y*-direction

Fig. 12 Time histories of the acceleration (soil)

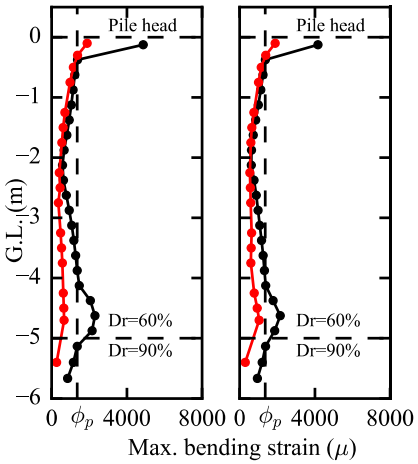

(a) *X*-axis (b) *Y*-axis

Fig. 13 Maximum bending strain of pile B2

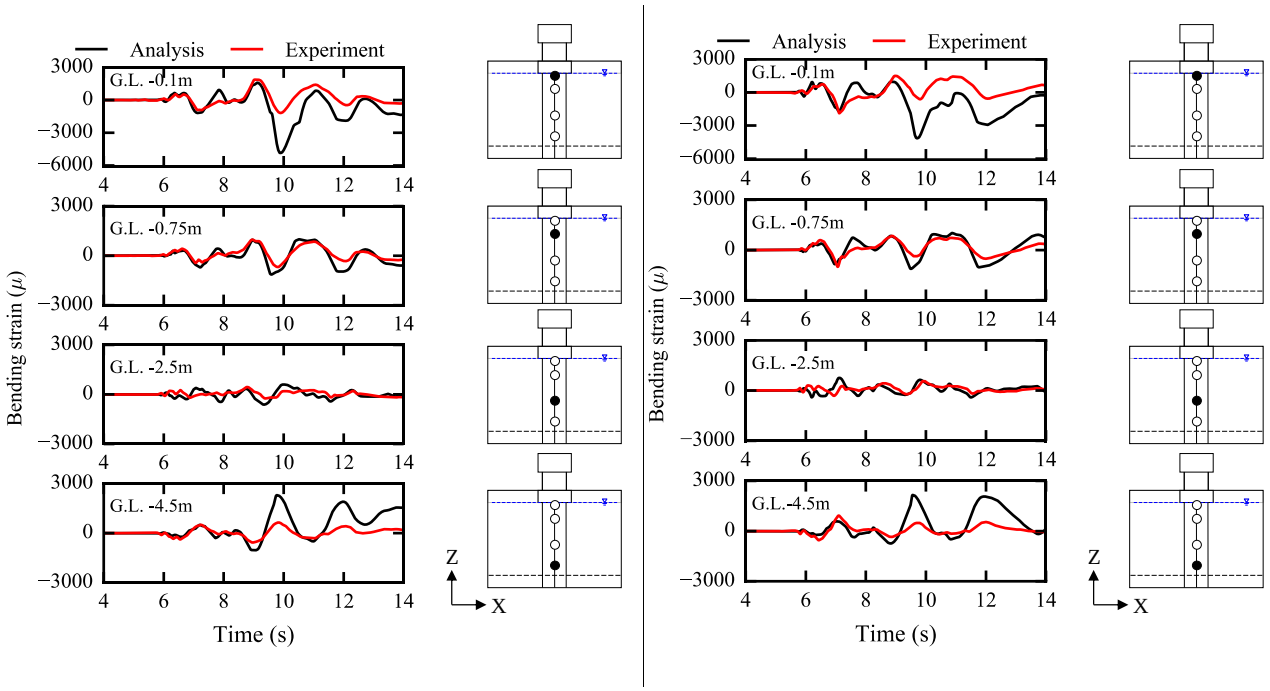

(a) *X*-axis (b) *Y*-axis

Fig. 14 Time histories of the bending strain of pile B2

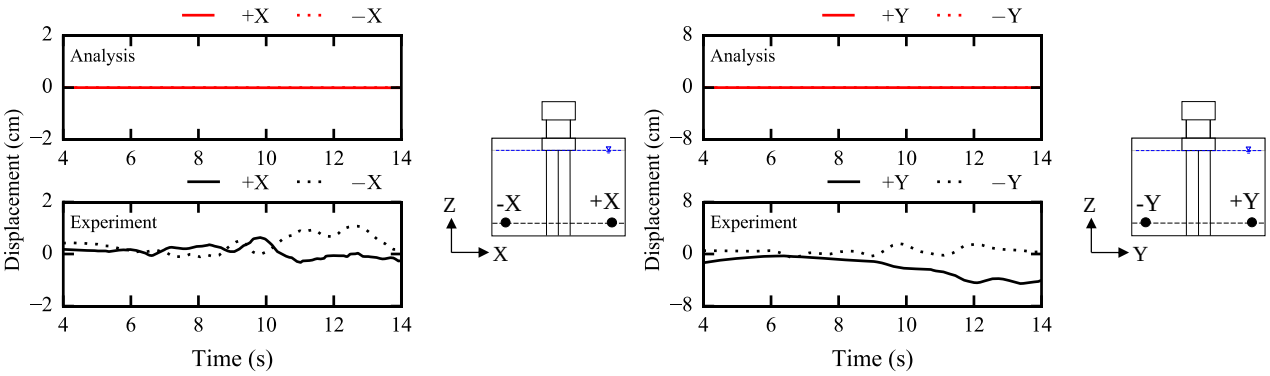

(a) *X*-direction (b) *Y*-direction

Fig. 15 Time histories of the vertical displacement

4. Conclusions

In this paper, a 3D liquefaction analysis of a soil-pile-structure system was conducted to validate the 3D FEM model. The results of the analysis were compared with the experimental data of a large scale shaking table test that was conducted in E-Defense. Although inconsistency of bending strains was found at pile heads, it was shown that the 3D FEM model can satisfactorily reproduce the experimental data in terms of acceleration, displacement, and pore water pressure which were densely measured. Thereby the validity of the 3D FEM model which was analyzed by FLIP 3D is demonstrated.

5. Acknowledgements

The study described herein was made possible through Special Project for Earthquake Disaster Mitigation in Urban Areas, supported by the Ministry of Education, Culture, Sports, Science and Technology (MEXT). The authors express their sincere thanks to the above organization.

6. Copyrights

7. References

[1] Kusakabe, R., Ichimura, T., Fujita, K., Hori, M., & Wijerathne, L. (2019). A finite element analysis method for simulating seismic soil liquefaction based on a large-scale 3D soil structure model. Soil Dynamics and Earthquake Engineering, Vol. 123, 64-74.

[2] Uzuoka, R., Sento, N., Kazama, M., Zhang, F., Yashima, A., Oka, F. (2007). Three-dimensional numerical simulation of earthquake damage to group-piles in a liquefied ground. Soil dynamics and earthquake engineering, 27(5), 395-413.

[3] Iai, S., Matsunaga, Y. and Kameoka, T. (1992): Strain space plasticity model for cyclic mobility, Soils and Foundations, Vol.32, No.2, 1-15

[4] Iai, S., Ozutsumi, O (2005): Yield and cyclic behaviour of a strain space multiple mechanism model for granular materials. International Journal for Numerical and Analytical Methods in Geomechanics, Vol. 29,417-442.

[5] Suzuki, H., Tokimatsu, K., Tabata, K. (2014). Factors affecting stress distribution of a 3× 3 pile group in dry sand on three-dimensional large shaking table tests. Soils and Foundations, 54(4), 699-712.

[6] Suzuki, H., Tokimatsu, K., Sato, M., Tabata, K. (2008). Soil-pile-structure interaction in liquefiable ground through multi-dimensional shaking table tests using E-Defense facility. In 14th World Conference on Earthquake Engineering, Beijing, China.

[7] P.R. Amestoym, I.S. Duff, J.-Y L'Excellent (2000): Multifrontal parallel distributed symmetric and unsymmetric solvers, Comput. Meth. Appl. Mech. Eng., Vol.184, 501-520.

[8] Yoshida, H., Zhou, K., Suzuki, H., Nukui, Y., Tokimatsu, K. (2010). Simulation of soil-pile-structure interaction through multi-dimensional shaking table tests using E-Defense facility. In 7th International Conference on Urban Earthquake Engineering, Tokyo, Japan.

[9] Zhou, Y., Tokimatsu, K., Suzuki, H., Yoshida, H., Nukui, Y. (2012). Numerical Study of Three-Dimensional Nonlinear Behavior of Soil-Pile-Structure System under Strong Input Motion. In Proceedings of the 15th World Conference on Earthquake Engineering, 24-28.

